Defence Science Journal, Vol. 58, No. 3, May 2008, pp. 315-326

Design and Simulation of Blending Function for Landing Phase of a UAV

K. Senthil Kumar, C. Sudhir Reddy, and J. Shanmugam

Madras Institute of Technology (MIT), Anna University, Chennai-600 044

ABSTRACT

This paper aims to achieve the autonomous landing of unmanned air vehicle (UAV). It mainly deals with glide path design, flare path design, design of blending function, and interfacing the glide and flare paths with the blending function. During transition from glide slope to flare path, a UAV will tend to the unstable region. In a manned aircraft, the pilot controls the unstability that occurs during the change of phase from glide slope to flare, but which is impossible in UAV till now. A blending function has been formulated for use in a UAV to overcome this unstability during transition. This simulation is done with the Matlab Simulink and the results are reported.

Keywords: UAV, landing phase, glide slope, flare path, blending function, simulation, unmanned air vehicle

1. INTRODUCTION

Over the past few decades, a keen interest is growing for the development of flying objects of small size for a variety of civilian and military applications. An unmanned autonomous aerial vehicle can perform tasks which would be exceedingly difficult or hazardous for a manned vehicle. Possible applications of this technology include search, rescue, surveillance, aerial mapping, inspection of structures like bridges and power lines, particularly in environmental conditions where human guided flights are not possible. The strategic importance of their use as reconnaissance aircraft is easily understood. Various attempts have been made to automate the control of an aerial flying vehicle. An unmanned air vehicle (UAV) is expected to complete the mission and return to the base in an autonomous manner. The recovery of a UAV is the most challenging and hazardous part of a UAV's flight.

2. PROBLEM STATEMENT

In this paper, an attempt has been made to design and simulate the blending function for landing phase of a UAV. The landing phase is divided into two parts, viz; glide path and flare path. The problem faced during the transition from glide path to flare is clearly addressed in this paper. A new concept termed as blending function during the transition region is discussed and a possible solution is suggested. Flying aircraft are subject to wind disturbances[1,2] that can be fatal when these occur close to the ground while landing. However, this problem is not addressed in this paper due to autoland systems that are routinely employed are not designed to handle large wind gusts that occasionally occur.

3. DESIGN OF BLENDING FUNCTION

The blending function is mixing of signals during the transition from glide path[3-8] to flare path [3-7,9].

Received 06 February 2007, revised 24 July 2007

This function is conceived to solve the problem of extreme oscillations and instability during the transition period. The proposed geometry of blending function is shown in Fig.1. In the blending function, the gain of glide and flare paths is varied according to variation in range. It is observed that the glide path gain is decreasing and the flare path gain is increasing. By using a limiter, the upper limit of the gain is set to 1 and the lower limit is set to 0. At any point the sum of the glide and the flare path gain is 1. From range R_1 to R_3, the glide path alone will be present, the gain of the glide path is 1 and the flare path gain is 0. From R_2 to 0 only the flare path will be present, the glide path gain is 0 and the flare path gain is 1. In between R_3 and R_2 the blending function will occur and the gain will vary with glide path gain decreasing from 1 to 0 and flare path gain increasing from 0 to 1. The conditon of the range is ($R_1 > R_3 > R_2 > 0$). Here, R_1 is the point from which glide path starts; G_{g1} is the gain at which glide path starts; R_2 is the range at which glide path gain becomes zero; R_3 is the range at which flare path gain becomes zero; and G_{f1} is the flare path gain at R_1.

The equation of straight line with coordinates (x_1, y_1) and (x_2, y_2) is given by

$$(y - y_1) = \frac{y_2 - y_1}{x_2 - x_1}(x - x_1) \tag{1}$$

such that the glide path gain equation with the coordinates (R_1, G_{g1}) and $(R_2, 0)$ as

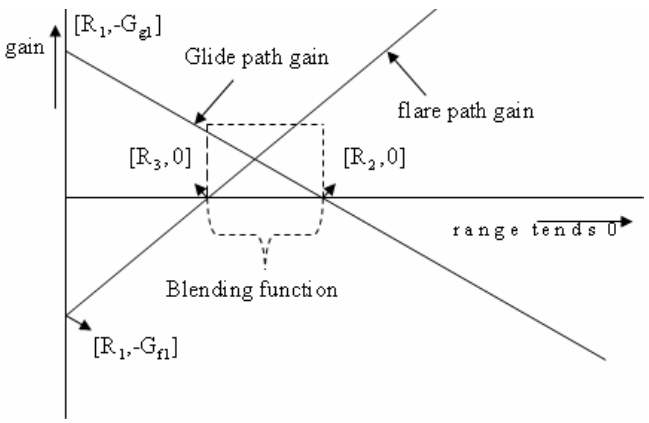

Figure 1. Geometry of blending function.

$$G_g - G_{g1} = \frac{0 - G_{g1}}{R_2 - R_1}(R - R_1) \tag{2}$$

$$= \frac{-G_{g1}}{R_2 - R_1}(R - R_1) \tag{3}$$

$$= \frac{G_{g1}}{R_2 - R_1}(R_1 - R) \tag{4}$$

$$G_g = \frac{G_{g1}}{R_2 - R_1}(R_1 - R) + G_{g1} \tag{5}$$

where G_g is the Glide path gain at every instant of range R, and the flare path gain equation with the coordinates $(R_1, -G_{f1})$ and $(R_3, 0)$ as

$$G_f - G_{f1} = \frac{0 + G_{f1}}{R_3 - R_1}(R - R_3) \tag{6}$$

$$= \frac{G_{f1}}{R_3 - R_1}(R - R_3) \tag{7}$$

$$G_f = \frac{G_{f1}}{R_3 - R_1}(R - R_3) + G_{f1} \tag{8}$$

where G_f is the flare path gain at every instant of range R.

In the region between range R_3 and R_2 the blending phenomenon will occur.

4. MATLAB IMPLEMENTATION OF BLENDING FUNCTION

Here R_2=3000; R_3=5000; $G = \frac{1}{R_3 - R_2}$

The geometrical implementation of the blending equations using Matlab Simulink[11-13] is shown in Fig. 2 and the interfacing of blending function with the glide and flare paths is shown in Fig. 3.

5. RANGE AND HEIGHT CALCULATION

Figure 4 illustrates the geometry to find out the instantaneous range of UAV which mainly depends upon the latitude, longitude and altitude (LLA) of the UAV and the destination runway.

The latitude conversion to feet is relatively constant from the equator to the poles and is approximated at all points as 6076 ft/min. The longitude conversion to feet varies from the equator to the poles. This is because the lines of longitude become closer towards the poles. The circle created by intersecting a plane with the earth at some line of latitude will have a radius equal to the radius of the earth times the cosine of the latitude angle. The radius of this circle is used to calculate the circumference of the earth at that particular latitude. Regardless of the circumference of the circle, it still contains 360^0, thus a conversion factor can be calculated. The website www.earth.google.com[14] provides commonly used constants, conversion factors and measurements. Google earth provides the average radius of the earth as 36,522 ft. This then yields the conversion factor for longitude as 36,522*cos(latitude^o) ft/min.

The steps involved for LLA calculation are:

(i) known parameteres are airport latitude, airport longitude, base elevation of the runway and initial ground distance from which glide path starts,

(ii) based on range, height of aircraft above base elevation are calculated, and

(iii) the aircraft LLA is calculated as:

$$Gd_{ini} \times \cos\left(\frac{\pi}{180} \times T_{head}\right) \times \frac{1}{6076 \times 60} + Lat_{initial} = lat_{Threshold} \quad (9)$$

$$\frac{Gd_{ina} \times \sin\left(\frac{\pi}{180} \times T_{head}\right) \times \frac{1}{6076 \times 60}}{\cos\left(\frac{\pi}{180} \times lat_{Initial}\right)} + Lon_{initial} = lon_{Threshold} \quad (10)$$

$$\text{Base elevation} = alt_{Threshold} \quad (11)$$

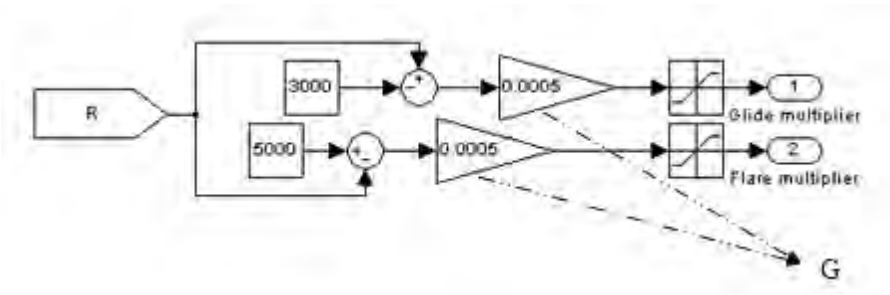

Figure 2. Blending function.

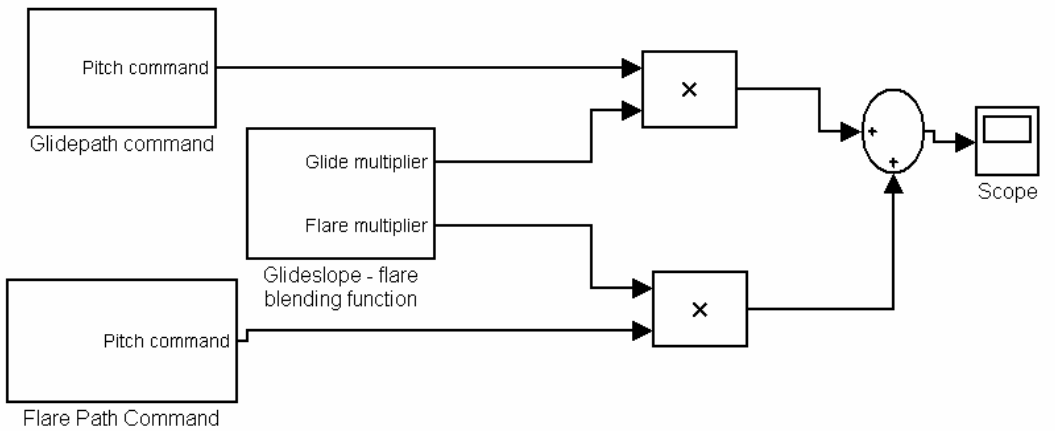

Figure 3. Interfacing of blending function with glide and flare paths.

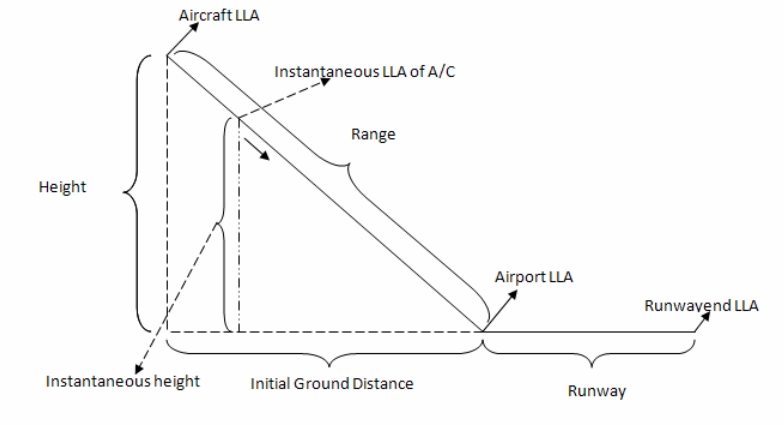

Figure 4. Latitute, longitude, and altitude calculations.

$$\text{alt}_{\text{Initial}} = \text{h}_{\text{Initial}} + \text{Base elevation} \quad (12)$$

(iv) the runway end LLA is calculated as

$$\left[\begin{array}{l}[\{\text{Gd}_{\text{ina}} + \text{Runway length}\} \\ \times\cos(\frac{\delta}{180}\times \text{T}_{\text{head}})\times\frac{1}{6076\times 60}]+\text{lat}_{\text{Initial}}\end{array}\right] = \text{lat}_{\text{Runwayend}} \quad (13)$$

$$\left[\frac{[\text{Gd}_{\text{ina}} + \text{Runway length}\}\times\sin(\frac{\delta}{180}\times \text{T}_{\text{head}})\times\frac{1}{6076\times 60}]}{\cos(\frac{\delta}{180}\times \text{lat}_{\text{Initial}})} + \text{lon}_{\text{Initial}}\right] = \text{lon}_{\text{Runwayend}} \quad (14)$$

$$\text{Base elevation} = \text{alt}_{\text{Runwayend}} \quad (15)$$

(v) instantaneous range and height is calculated as:

$$\sqrt{\begin{array}{l}[\text{lat}_{\text{Threshold}} - \text{lat}_{\text{Initial}}]\times 6076\times 60]^2 + \\ \left[\begin{array}{l}[\text{lon}_{\text{Threshold}} - \text{lon}_{\text{Initial}}]\times 6076\times 60\times \\ \cos(\frac{\pi}{180}\times \text{lat}_{\text{Initial}}\end{array}\right]^2 + \\ [\text{alt}_{\text{Threshold}} - \text{alt}_{\text{Initial}}]^2\end{array}} = \text{range}_{\text{initial}} \quad (16)$$

$$\sqrt{\begin{array}{l}[[\text{lat}_{\text{Ins}} - \text{lat}_{\text{Initial}}]\times 6076\times 60]^2 + \\ \left[\begin{array}{l}[\text{lon}_{\text{Ins}} - \text{lon}_{\text{Initial}}]\times 6076\times 60\times \\ \cos(\frac{\pi}{180}\times \text{lat}_{\text{Initial}})\end{array}\right]^2 + \\ [\text{alt}_{\text{Ins}} - \text{alt}_{\text{Initial}}]^2\end{array}} = \text{range}_{\text{Delta}} \quad (17)$$

$$\text{range}_{\text{Initial}} - \text{range}_{\text{Delta}} = \text{range}_{\text{Ins}} \quad (18)$$

$$\text{alt}_{\text{Ins}} - \text{Base elevation} = \text{h}_{\text{Ins}} \quad (19)$$

The symbol and description of the various parameters used in the equations are given below:

Symbol	Description	Symbol	Description
Gd_{ini}	Initial ground distance	T_{head}	True heading
$\text{Lat}_{\text{initial}}$	Initial latitude	$\text{lon}_{\text{initial}}$	Initial longitude
$\text{alt}_{\text{initial}}$	Initial altitude	$\text{lat}_{\text{Threshhold}}$	Threshold latitude
$\text{lon}_{\text{threshhold}}$	Threshold longitude	$\text{alt}_{\text{Threshhold}}$	Threshold altitude
$\text{lat}_{\text{runwayend}}$	Runwayend latitude	$\text{lon}_{\text{Runwayend}}$	Runwayend longitude
$\text{alt}_{\text{runwayend}}$	Runwayend altitude	$\text{range}_{\text{initial}}$	Initial Range
$\text{Range}_{\text{Delta}}$	Change in range	$\text{range}_{\text{ins}}$	Instantaneous height
$\text{h}_{\text{initial}}$	Initial height	h_{ins}	Instantaneous height

5.1 Sample Calculation

In this paper, the Dallas Fort Worth International Airport has been considered for the landing phase of UAV with the following known parameters: True heading of 180.3 deg, base elevation of 607 ft, latitude of 2.93483568652165 deg, longitude of – 97.0268825156042 deg and Initial ground distance of 24300 ft. These values are used to calculate initial range, instantaneous range, initial height and instantaneous height. Using steps (iii) to (v), the calculated values are:

Initial height = 1060.960 ft

Initial altitude = 1667.96 ft

Initial latitude = 33.00149046735776°

Initial longitude = – 97.0272315271941°

Runway-end altitude = base elevation = 607 ft

Runway length = 6076 ft

Runway-end latitude = 32.91816924831753°

Runway-end longitude = – 97.0267952483441°

Initial range = 24323.1502096 ft

Delta range = 6361 ft

Instantaneous range = 24323.1502096–6361=17962 ft

With simulation run in Matlab Simulink environment for about 20 s, it is observed that the simulated instantaneous range is equal to the calculated instantaneous range. Hence, it has been proved that the algorithm is more efficient and this has been verified with many more airports around the world.

6. SIMULATION RESULTS

6.1 Gain Variation with Range

The simulation input namely latitude, longitude and altitude are given from the airport selector function and these values are used to calculate the range. The simulation results are shown in Figs 5–8. In Fig. 5, the range, glide multiplier gain and flare multiplier gain variation with time is shown. At the glide starting point, the range is around 23,000 ft and by the time it reaches 86 s, the range is 0 ft. This implies that landing has been accomplished. Table 1 describes the gain variation with range starting from glide slope to touch down point.

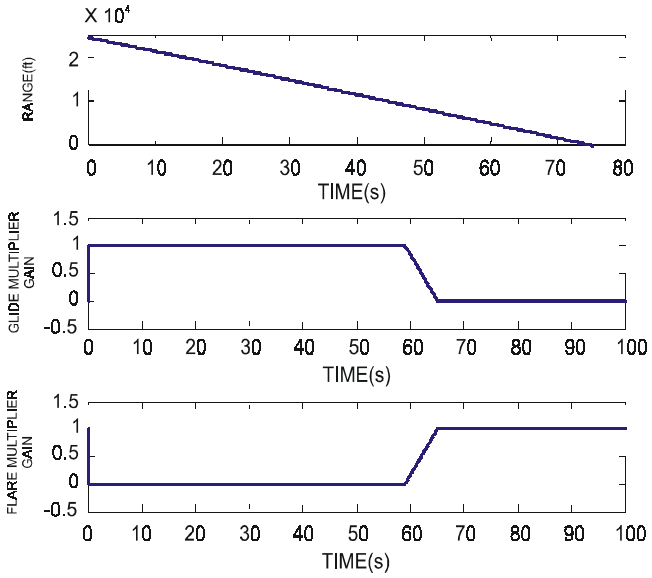

Figure 5. Response of range, glide multiplier gain, and flare multiplier gain.

Figure 6 shows the variation of the glide multiplier gain with range and it is observed that from glide slope starting point, i.e., 23,000 ft to 5000 ft, the gain remains as 1 between 5000 ft and 3000 ft, the gain gradually decreases from 1 to 0 and from 3000 ft to touch-down point, the gain decreases to 0. Figure 7 shows that the flare multiplier gain varies from 0 to 1. The flare starting point is 5000 ft and up to that point, the gain is 0, and from 3000 ft to touch-down point the gain remains as 1. It means that in the flare path between 5000 ft and 3000 ft, the gain is increasing from 0 to 1. It is observed from Figs 6 and 7 that between 5000 ft and 3000 ft, the glide path gain is decreasing, the flare path gain is increasing, and the blending phenomenon is said to occur. From Fig. 8, it is inferred that the summation of the glide and flare path gain always remains as 1.

Table 1. Gain variation with range

Range (ft)	Glide path gain	Flare path gain
23000–5000	1	0
5000–3000	1→ 0	0 → 1
3000–0	0	1

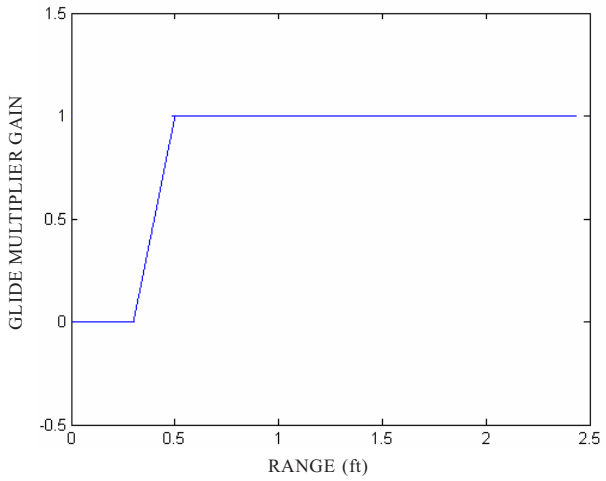

Figure 6. Glide multiplier gain versus range.

6.2 Response of the Parameters Variation without Blending Function

The responses of the various parameters without using blending function are shown in Figs 9-15.The flare path starts at 3000 ft, above 3000 ft glide path alone will be present. In terms of time, upto 65 s only glide path will be present and after 65 s the flare path alone will be present.

From Fig.15 it can be observed that during transition from glide slope to flare path, the UAV will experience large variation warranting more deflection in the elevator command which is not recommended during this transition.

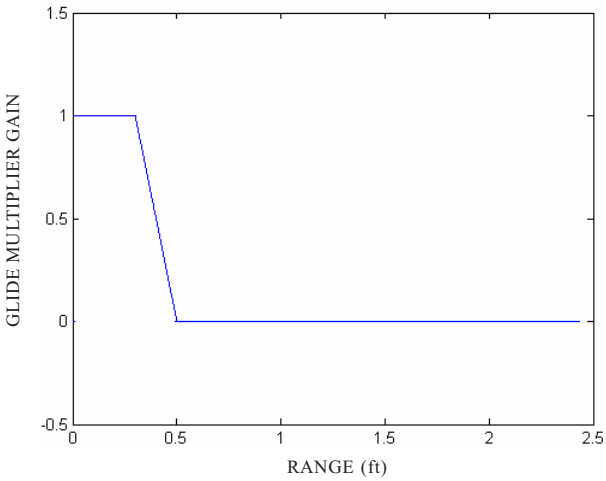

Figure 7. Flare multiplier gain versus range.

6.3. Responses of the Parameters Variation with Blending Function

The responses of the various parameters with the blending function are shown from Figs 16–22. The blending phenomenon occurs from 5000 ft to 3000 ft, which means that between 5000 ft and 3000 ft the UAV will be in both glide path and flare path. Above the altitude of 5000 ft (i.e., from 23000 ft to 5000 ft) the UAV will be

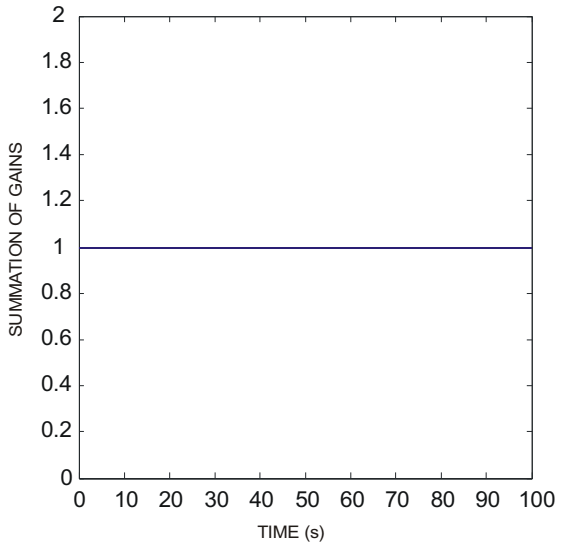

Figure 8. Summation of gains.

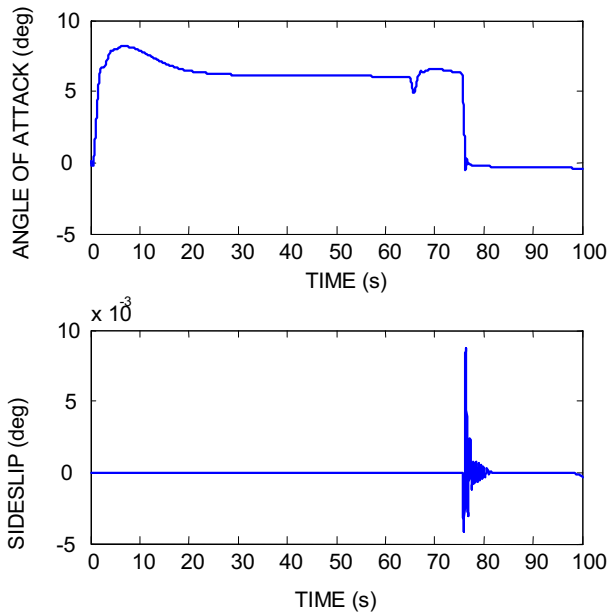

Figure 9. Responses of angle of attack and side slip.

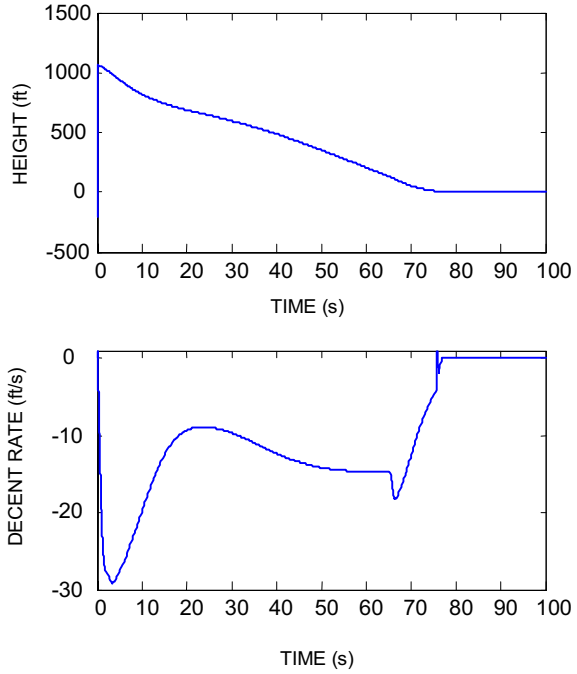

Figure 10. Responses of height and decent rate.

in the glide path and below the altitude of 3000 ft (i.e., from 3000 ft to touch-down point), it will be in the flare path only. In terms of time, the blending phenomenon will occur between 59 s and 65 s. During 0–59 s, only the glide path will be present and after 65 s, only the flare path will be present.

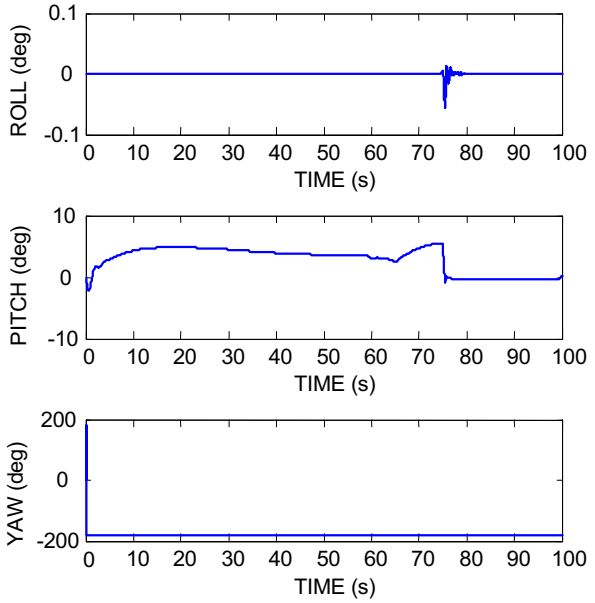

Figure 11. Responses of pitch, roll, and yaw angles.

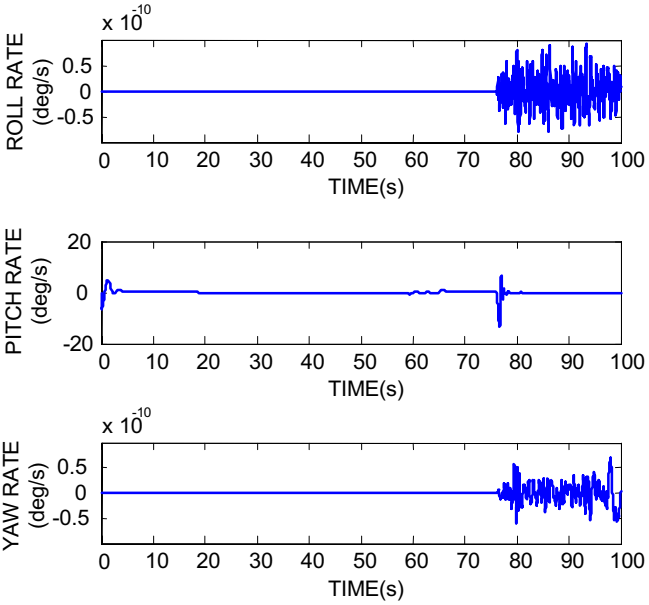

Figure 12. Responses of yaw rate, pitch rate, and roll rate.

7. COMPARISON OF PERFORMANCE WITH AND WITHOUT BLENDING FUNCTION

The Figs 23–30 show the comparison of angle of attack, sideslip, height, pitch rate, roll rate, and yaw rate with and without blending function. The dotted lines indicate the parameter variation with blending function and thick lines indicate the parameter variation without blending function. The parameters are compared with range variation.

From 5000 ft to 3000 ft with time variation from 59 s to 65 s, the angle of attack variation with

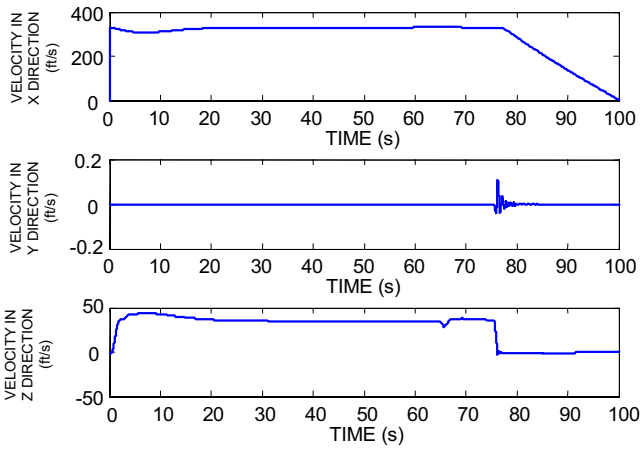

Figure 13. Responses of aircraft velocity in *x*, *y*, and *z* directions.

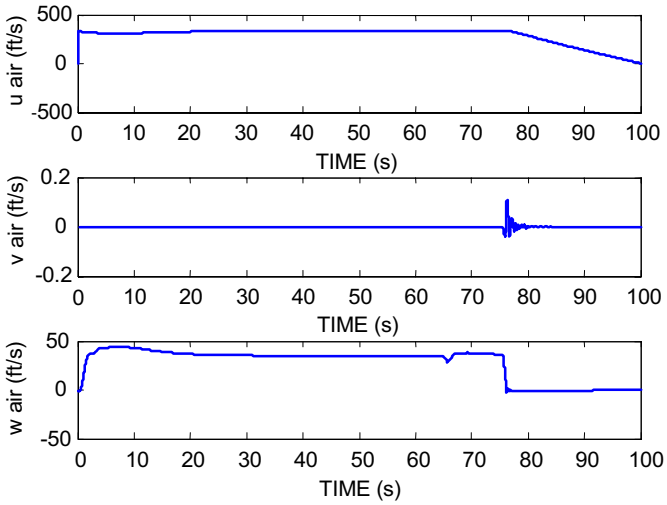

Figure 14. Responses of air velocities in x, y and z directions.

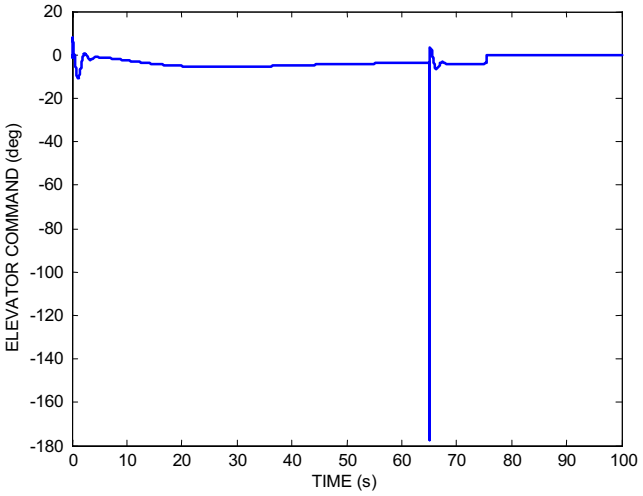

Figure 15. Response of elevator command.

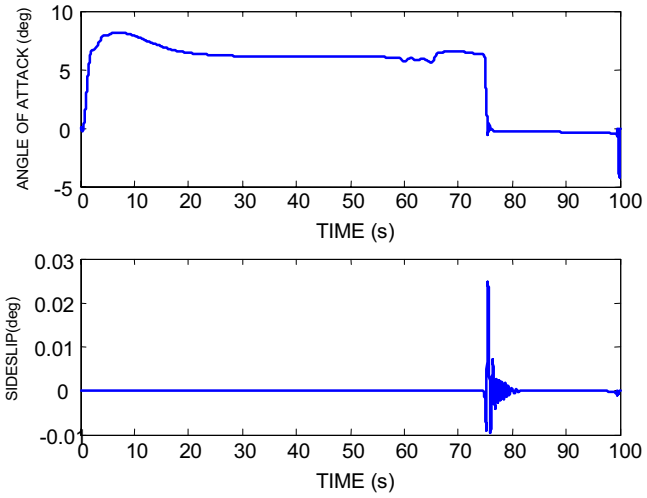

Figure 16. Responses of angle of attack and side slip.

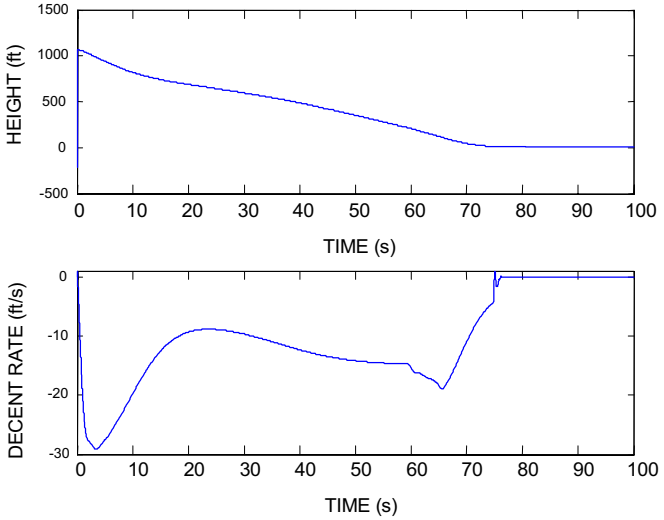

Figure 17. Responses of height and decent rate.

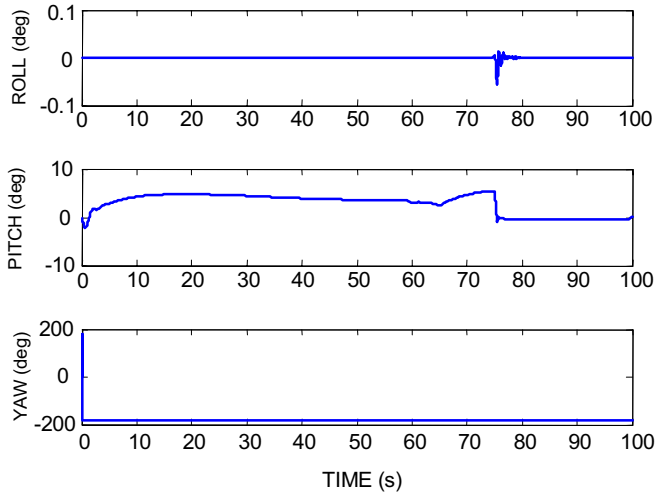

Figure 18. Responses of roll, pitch, and yaw angles.

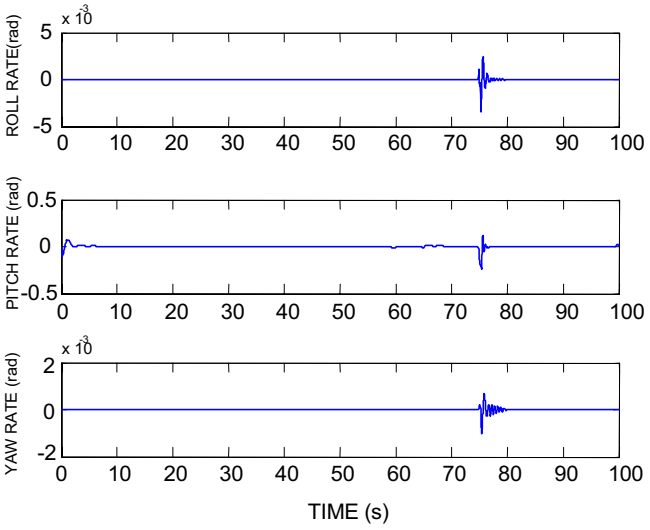

Figure 19. Responses of yaw rate, pitch rate, and roll rate.

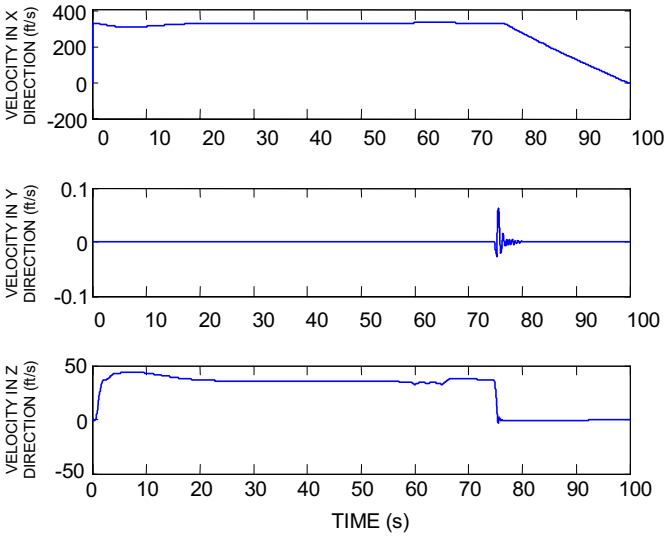

Figure 20. Responses of aircraft velocites in *x*, *y*, and *z* directions.

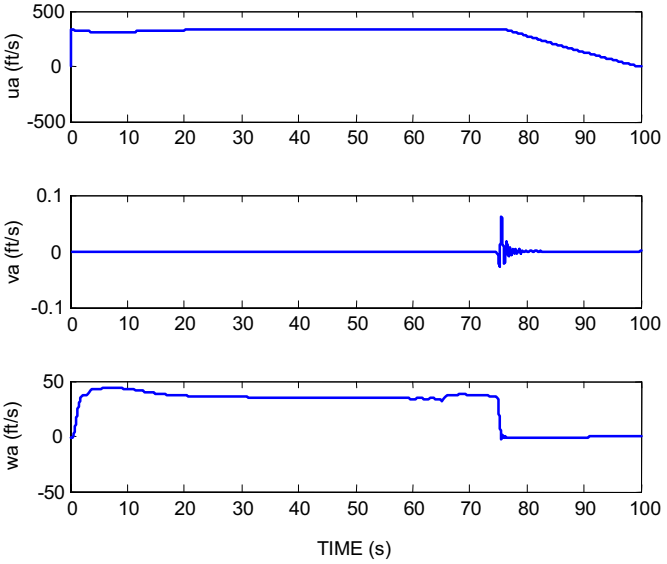

Figure 21. Responses of air velocity in *x*, *y*, and *z* directions.

and without blending function is as shown in Fig. 23. On comparison, it is observed that when the blending function is not included, the variation is large, i.e., around 15 per cent, but when the blending function is included, the variation is reduced to about 3 per cent.

The decent rate shown in Fig. 24 is smoother with the blending function than when compared to without the blending function. The smooth variation of decent rate means that when the oscillations get reduced, the steepness will also get reduced.

The comparison of heights shown in Fig. 25 proves that the steepness of the aircraft is reduced. The exponential decay is found to be good when including blending function. If the steepness increases, i.e., without blending function, the force on the landing gear will also be increased. This may cause the landing gear failure and wear of tires, which makes the landing of the aircraft difficult.

On comparing the pitch rate as shown in Fig. 26, it is observed that the variation and the oscillations are considerably more when the blending function is not included. The variations are reduced when the blending function is included.

The comparison of pitch is shown in Fig. 27. It is observed that the instant pitch is available by

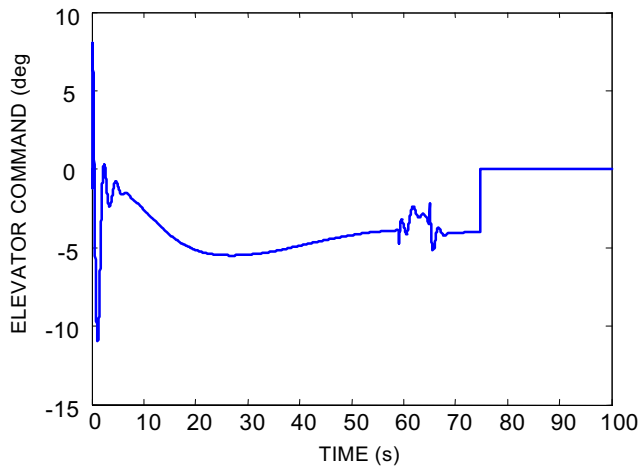

Figure 22. Response of elevator command.

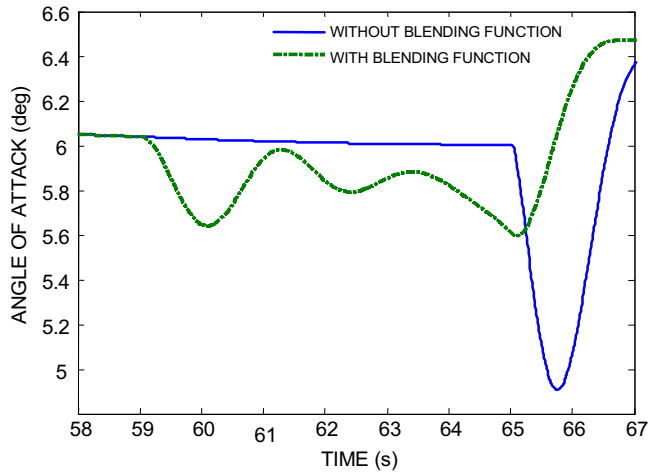

Figure 23. Response of angle of attack.

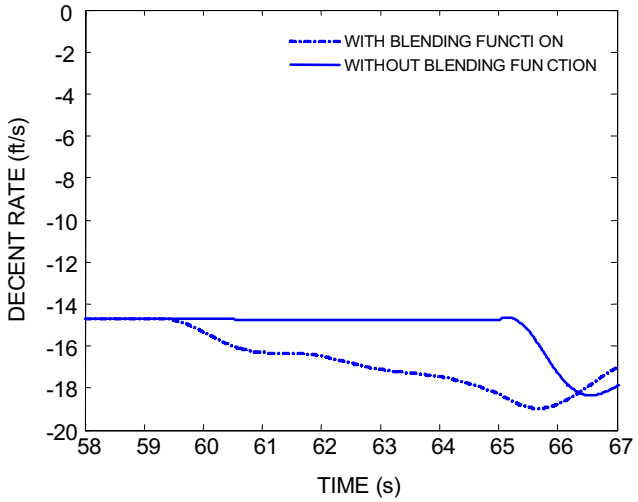

Figure 24. Response of decent rate.

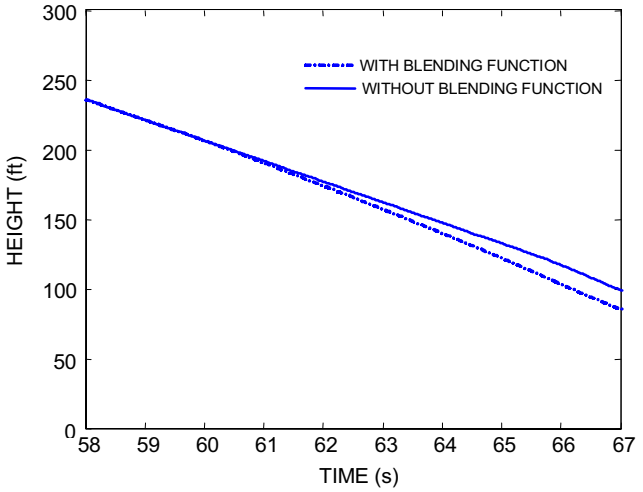

Figure 25. Response of height.

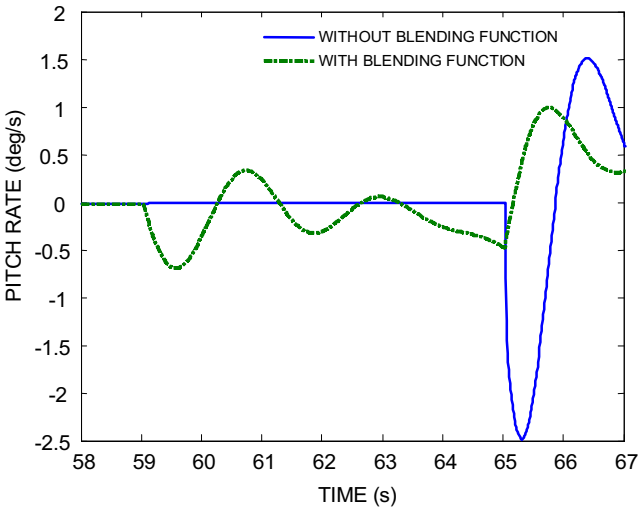

Figure 26. Response of pitch rate.

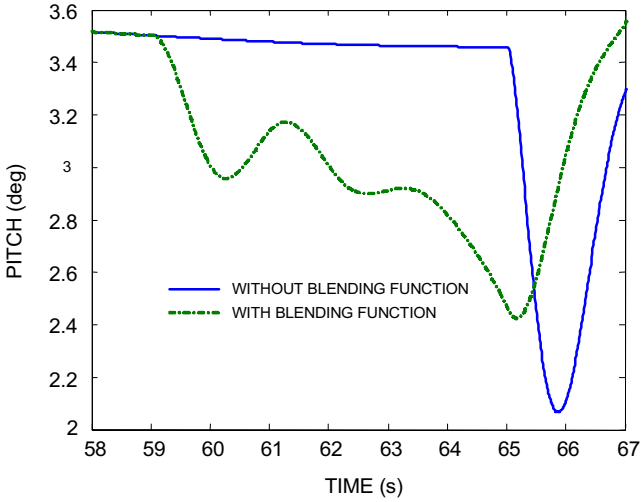

Figure 27. Response of pitch.

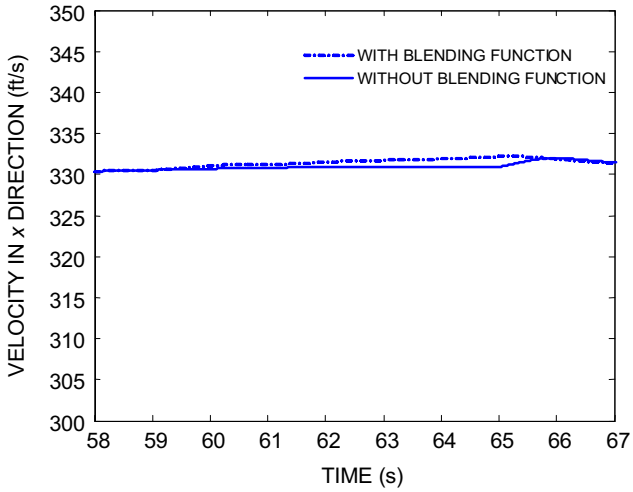

Figure 28. Response of velocity in *x*-direction.

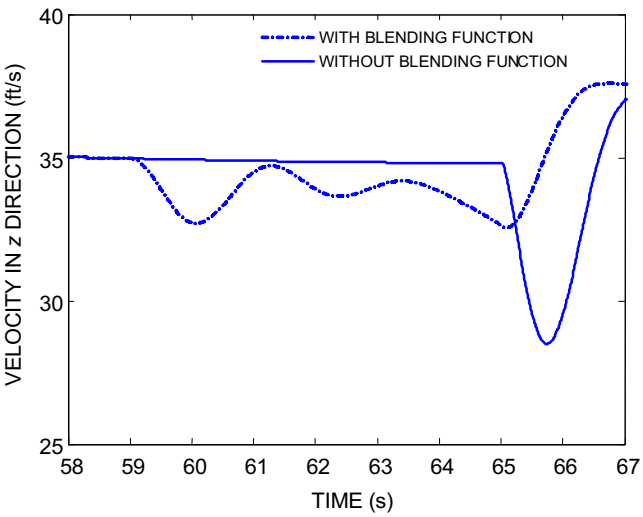

Figure 29. Response of velocity in *z*-direction.

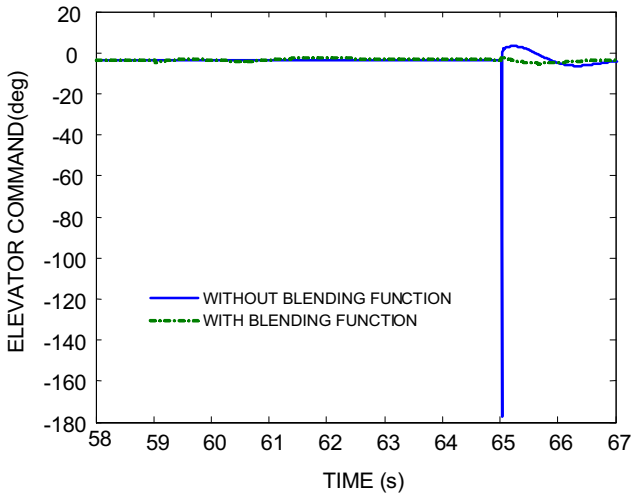

Figure 30. Response of elevator command.

summing the pitch at the previous instant and the pitch rate at that instant. Hence, when the pitch rate varies, the pitch will also vary automatically.

The variation of velocities wrt x- and z-directions are shown in Fig. 28 and Fig. 29 respectively with and without the blending function. The blending function ensures reduced velocity in z -direction which will cause smooth contact of the wheels with surface on touch down.

The elevator command, which is given to the elevator, is shown in Fig. 30, with and without blending function. The elevator deflection seems to be more when the blending function is not used, requiring more control power which might cause damage to control surface, resulting in fatal accidents during landing. Using the blending function, the control power required to move the elevator is substantially reduced.

Thus, using blending function, the oscillations are reduced and the control power is also considerably reduced as evident from the graph and ensures safe landing.

Table 2. Performance measures

Parameter	Without blending function	With blending function
Angle of attack	Variation is high	Variation is low
Decent rate	Sudden change	Smooth change
Height	Steepness is high	Steepness is low
Pitch rate	Variation is high	Variation is low
Pitch	Variation is high	Variation is low
Forward velocity in x-direction	Variation is not smooth	Variation is smooth
Forward velocity in z-direction	Variation is high	Variation is low
Elevator command	High deflection	Small deflection

Table 3. Typical values of performance measures

Parameters	At the glide slope begin (0 s)	At the start of blending function (59 s)	At the end of blending function (65 s)	At touch-down point (86 s)
Angle of attack (deg)	2	6	5.6	– 0.3
Sinkrate (ft/s)	20.8	14.71	– 18.6	– 0.001
Altitude (ft)	1074	221	123	7.5
Pitch rate (deg/s)	3.7	– 0.014	– 0.5	0
Pitch angle (deg)	0.5	3.5	2.5	– 0.3
Incremental forward velocity (ft/s)	325	330	332	184
Incremental vertical velocity (ft/s)	12	35	32.6	– 1
Throttle	0.045	– 0.06	0.2466	0.1
Elevator command (deg)	0.18	0.2696	– 0.06	0
Range (ft)	24330	5000	3000	0

8. COMPARISON OF PERFORMANCE MEASURES

Measures of performance[6] are required to specify the desired landing conditions of aircraft. Basically, they require that the aircraft must land within the desired envelope of dispersions. Table 2 summarises the blending performance measures.

9. CONCLUSIONS

In the present study, a blending function has been formulated for use in an UAV using simulation with Matlab Simulink. From the simulation results, it is inferred that the blending of signals during transition from glide slope to flare solves the problem of unstability and extreme oscillations. The property of the blending function has proved that the summation of the gains is always equal to 1. It is evident that the landing of the UAV using blending function gives good performance measures.

ACKNOWLEDGMENTS

The authors would like to express their sincere thanks and gratitude to Dr P.A. Janaki Raman, Professor, Dept of Electrical Engineering, Indian Institute of Technology Madras, Chennai; Shri P.S. Krishnan, Director Aeronautical Development Establishment, Bangalore; and Shri K.V. Srinivasan, Scientist G, ADE, Bangalore, for their inspiration and encouragement for successful completion of this work.

REFERENCES

1. Ih-Gau, Juang & Jern-Zuin, Chio. Fuzzy modeling control for aircraft automatic landing system. *Int. J. Syst. Sci.*, 2005, **36**(2), 77-87.
2. Neuman, F. & Foster, J.D. Investigation of a digital automatic aircraft landing system in turbulence. NASA Ames Research Center, Moffet Field, CA.,1970, NASA-TND-6066.
3. Yong,Tao. & Yongzhang, Shen. Guidance and control for automatic landing of UAV. *Trans. Nanjing Univ. Aero. Astro.*, 2001, **18**(2), 229-35.
4. Blakelock, J.H. Automatic control of aircraft and missiles. John Wiley Sons, NY., 1990.
5. McLean, Donald. Automatic flight control systems. Prentice-Hall Publications, 1990.
6. Senthil Kumar, K.; Shanmugam, J. & Srinivasan, K.V. Neural network approach for autopilot and landing phase of unmanned air vehicle. *In* 1st Indian International Conference on Artificial Intelligence, 2003. pp. 1028-037
7. Li,Y.; Sundararajan, N.; Saratchandran, P. & Wang, Z. Robust neuro-H8, controller design for aircraft auto-landing. *IEEE Trans. Aero. Elec. Syst.,* 2004, **40**(1), 158-67.
8. Senthil Kumar, K.; Reddy, Sudhir C. & Shanmugam, J. Design of glide slope control system for landing phase of large unmanned aerial vehicle. *In* Proceedings of the International Conference on High Speed Transatmospheric Air and Space Transportation, 29-30 June 2007, Hyderabad, Aeronautical & Astronautical Societies of India, pp. 99-108
9. Charles, C.; Jorgensen & Schley, C. A neural network baseline problem for control of aircraft flare and touch-down, edited by W. Thomas Miller lll; Richard S. Sutton and Paul J. Werbos. pp. 403-25.
10. Pasko, G.; Pasko, A. & Kunii, T. Bounded blending for function-based shape modelling, Pre-final version before editing by the IEEE CG&A. pp. 36-45.
11 MAT LAB *User's Manual User's Guide*. The Math Works Inc, 2004.
12. Simulink User's Manual User's Guide. The Math Works Inc, 2004.
13. Control System Toolbox User's Manual. The Math Works Inc, 2004.
14. http://www.earth.google.com